Aust. J. Phys., 1991, **44**, 87–100

Lunisolar Atmospheric Tides. III*

R. Brahde

Institute of Theoretical Astrophysics, University of Oslo,
P.O. Box 1029, Blindern, 0315 Oslo 3, Norway.

Abstract

In two earlier papers (Brahde 1988, 1989) the atmospheric tide in Oslo (Norway) was studied using pressure data for 23 continuous years. In the present paper a similar study based on pressure data from Batavia (now Jakarta in Indonesia, latitude 6°08′S, longitude 106°45′E) is presented. The result is that the tidal wave caused by the lunisolar tide is represented by a one-day and a half-day oscillation with mean amplitudes of 0·11 and 0·33 mb respectively. The amplitude spectrum reveals amplitudes of up to 1 mb of dynamic origin. The 'thermal' tide is also studied and the connection between the thermal and dynamic effects is discussed.

1. The Data

Copies of 'Observations made at the Royal Magnetical and Meteorological Observatory at Batavia' were obtained from the Nederlands Meteorologisch Institut and records of the air pressure for the 10 years 1913–22 were selected. The observations covered every hour local mean solar time, starting one hour after midnight.

The dataset therefore comprises 87 648 measured values, a number comparable to the 100 800 values in Oslo. The scale of the measurements was mm Hg minus 750, and they were published in monthly blocks. We copied the data into a computer file exactly in this form and they were tested for unavoidable mistakes. We prefer to start at midnight, and therefore a value for 0^h January 1, 1913 was extrapolated. The data were transformed to the millibar scale and rewritten in annual blocks. While the pressure at the northern station Oslo is mainly dominated by the weather (see for instance Brahde 1988, Part I, Fig. 13), a regular daily variation is characteristic for the tropical station Batavia.

2. Comparison with the Tidal Acceleration

An example of the data is shown in the upper part of Fig. 1. The regular 24-hourly and 12-hourly variation is characteristic. In the lower part we show the vertical component of the tidal acceleration (Part I, pp. 808–9) computed

* Part I, *Aust. J. Phys.*, 1988, **41**, 807–31; Part II, *Aust. J. Phys.*, 1989, **42**, 439–50.

0004-9506/91/010087$05.00

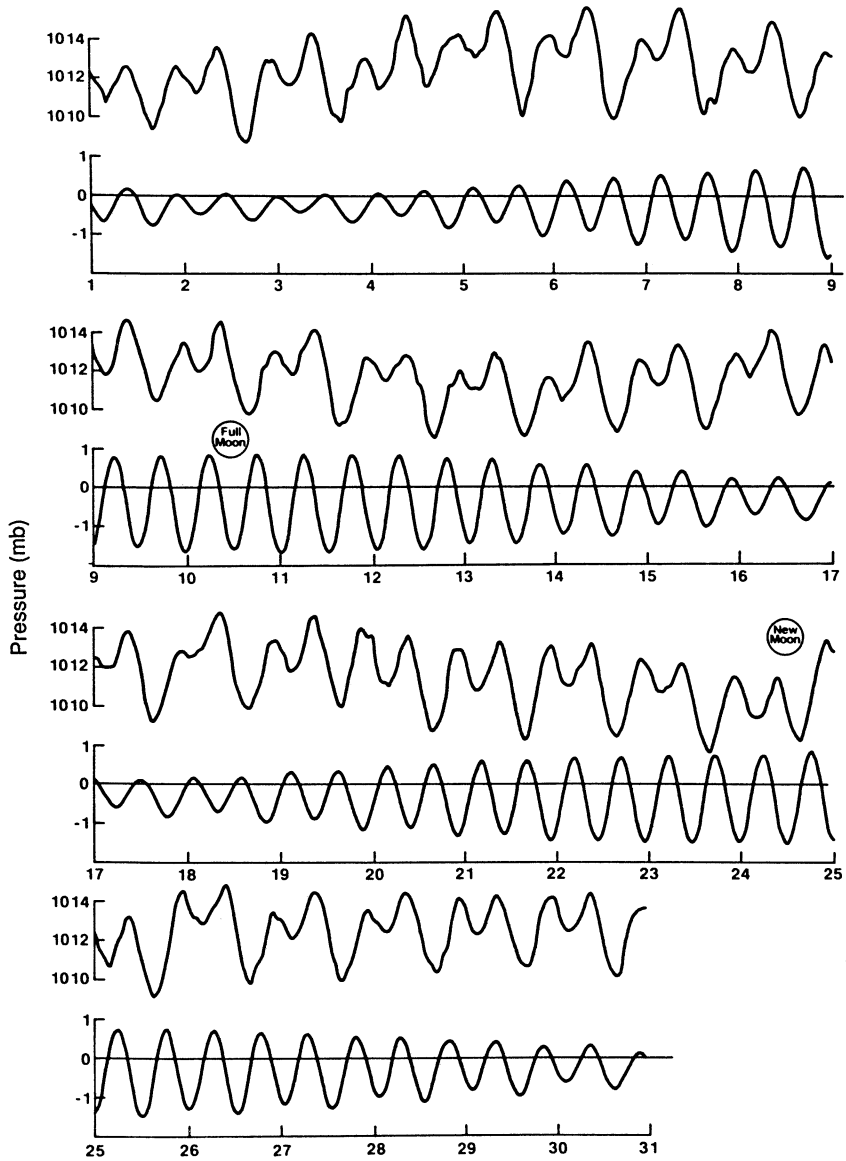

Fig. 1. Upper graph gives the observed pressure in Batavia during September 1919. The lower graph gives the computed values of the vertical component of the tidal acceleration (sign changed).

for the same times. The sign has been changes as before, and therefore the maxima of the acceleration correspond to the minima of the curve. This means that the curve shows the variation in gravity.

As a first attempt the correlation coefficient between the two series was formed. We selected data for each year, computed the coefficient, formed the mean and then found the standard deviation. We found a correlation coefficient of $-0 \cdot 107 \pm 0 \cdot 009$. However, if the pressure series is displaced relative to the

series of the acceleration, the result is different. When we compared the latter with the pressure measured one hour later it was $0 \cdot 004 \pm 0 \cdot 012$, two hours later it became $0 \cdot 113 \pm 0 \cdot 016$, three hours later, $0 \cdot 191 \pm 0 \cdot 021$, and a displacement of 4 hours resulted in a correlation coefficient of $0 \cdot 216 \pm 0 \cdot 025$. This is a maximum value, as a further displacement resulted in values diminishing to zero for 7 h, to $-0 \cdot 219$ for 10 h, then increasing to zero for 13 h and to a maximum of $0 \cdot 215$ for 16 h displacement. This shows that in spite of the obvious daily variation indicating a solar origin, there is a connection between the tidal acceleration and the pressure wave.

3. The Method

The method used in Part II was applied in order to find the dynamic component of the variation. Some changes had to be made because the present data were measured every hour instead of every 2 hours as in Oslo. Another difference is the shape of the curve of the vertical component. In Part I, Fig. 2 we noticed that the daily variation dominates, but for Batavia the half-day variation is by far the most conspicuous. This is because Batavia is a tropical station, only 6° south of the equator. In Part I it was emphasised that a station exactly on the equator would exhibit only the half-day variation. Therefore another change was made in the method: Instead of a comparison between the gradient of the pressure and the 'magnitude' of the acceleration defined by the difference between the primary maximum and the following minimum, we introduced two 'magnitudes', a primary and a secondary. Tidal noon was found as before to be the moment of primary maximum (the deepest minimum of the curve). Now the gradient during a tidal day was compared with the primary magnitude if it took place after tidal noon, and the gradients before tidal noon were compared with the secondary magnitude of the tidal day before.

With these changes the investigation was carried out as before. The vertical component of the combined lunar and solar tide was computed every half-hour. Maxima and minima were determined and the primary and secondary maxima were separated (minima of the lower curve in Fig. 1) (see also Part II p. 441). In Oslo at 60° northern latitude the primary maximum occurs during the day when the moon has a northern declination and during the night when it is south of the equator. In Batavia with a southern latitude, this is reversed.

The gradient of the pressure was determined as described in Part I, pp. 810–11, but now with 51 points in order to cover two days as before. (With one-hourly data this corresponds to the 25 values used in Parts I and II.) Similarly the noise was determined as before, and it was found that a noise limit of $0 \cdot 20$ mb was suitable. A small noise limit results in a smaller number of data points in the analysis, and therefore it was not chosen unnecessarily small. As a criterion we used the standard deviation of the gradient at each tidal hour. With a small number of data participating in the statistics the value varied appreciably from one tidal hour to the next, but with $\sigma = 0 \cdot 20$ or $0 \cdot 25$ the values became comparable. We formed the mean, and Table 1 shows the relation between the noise limit σ, the mean error of the gradient, and the number of data points participating. In the last row the noise limit 100 mb means that all data are included. The number 3513 in this case represents the

number of tidal days in the data. We would expect a total of 3652/1·0350502 or 3528 tidal days, but actually we lose some data when the moon crosses the equator and the shift between primary and secondary maxima takes place. According to Table 1 the smallest errors occur with a noise limit of 0·25 mb, but we preferred to use a value 0·20 mb which includes 96% of the data.

Table 1. The noise limit σ

σ (mb)	Mean error of gradient	Number of data points
0·10	0·0351	1425 (41%)
0·15	0·0172	2851 (81%)
0·20	0·0135	3374 (96%)
0·25	0·0125	3487 (99%)
100	0·1158	3513 (100%)

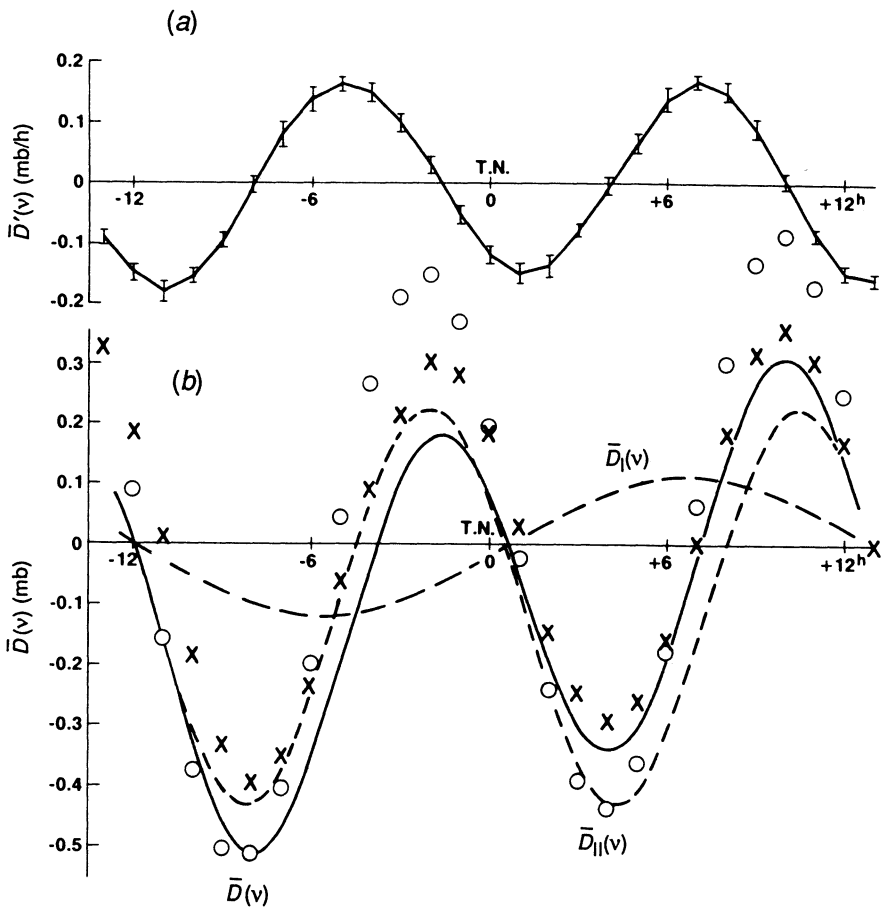

Fig. 2. (*a*) Mean pressure gradient $\bar{D}'(v)$ as a function of tidal phase. (*b*) Variation of mean dynamic pressure $\bar{D}(v)$ around T.N., showing its harmonic components $\bar{D}_I$ and $\bar{D}_{II}$. The circles represent the mean of the integrated values of the series $D(t)$ and the crosses show values with an improved classical method.

4. Dynamic Pressure Variation

In Fig. 2*a* we show the mean gradient of the pressure distributed through a tidal day. This figure corresponds to Fig. 4*a* in Part I and to the upper graphs of Fig. 1 in Part II. We notice that the amplitude is approximately doubled with the Batavia data, and that the half-day variation is prominent. The regularity of the Batavia data is also reflected in the much smaller error bars in Fig. 2*a*.

The Fourier method described in Part I, pp. 818–19 is used to integrate $\overline{D}'(v)$ to $\overline{D}(v)$. In order to find the period we studied the time intervals between adjacent T.N. values through the 10 years. If we exclude intervals of length around 12 and 36 hours occurring when primary and secondary maxima change position, we get a mean value of 1·0351, or a mean lunar day. However, by testing varying values for the period, it became evident that a scale of mean solar hours around tidal noon actually diminishes the oscillations of the higher modes 3–12. We found a one-day and a half-day oscillation with amplitudes 0·107 and 0·328 mb respectively. In Fig. 2*b* the resulting function $\overline{D}(v)$ is shown by the solid curve. The dashed curves show the one-day and the half-day modes. The sum of the higher harmonics gives variations of ±0·024 mb around a mean value 0·012 mb. Therefore the mean dynamic oscillation $\overline{D}(v)$ is well represented by the sum of the one-day and the half-day modes. We emphasise that in the determination of this curve we have used only the gradients determined from the data, in 13 steps of one hour on both sides of tidal noon.

5. The Series *D(t)*

In order to find the dynamical pressure variation through the 10 years we used the coefficient A_x in the regression equation $Y = A_x X$, where X is the magnitude of the acceleration, primary or secondary, and Y is the gradient of the pressure. The coefficient A_x has a minimum of −0·175 at T.N. -11^h, a maximum of 0·165 at T.N.-5^h, again a minimum of −0·143 at T.N.$+1^h$, and a second maximum of 0·150 at T.N.$+7^h$. The mean value of the 10 years was found for every hour during the tidal day. In addition the correlation coefficient between the 'magnitudes', primary or secondary, and the gradient was found.

It has a shape similar to A_x, but it varies between the limits −0·745 and +0·737 with a standard deviation of 0·023. It was computed in order to show the strong connection between the 'magnitudes' of the acceleration and the gradient of the atmospheric pressure. [This is important as the gradients were based solely on the pressure data arranged according to tidal hour, independent of the values of the acceleration. Therefore the numerically high values of the correlation coefficient, depending on the tidal phase, prove that the gradient $\overline{D}'(v)$ has a dynamic cause.]

We selected the time for each tidal noon in the list, formed 25 moments from T.N.-12^h to T.N.$+12^h$ and computed a series $D'(t)$ by means of the regression coefficient A_x and the primary or secondary 'magnitude' of the acceleration. In accordance with the determination of the coefficient, we used the primary magnitude if the gradient was obtained from T.N. to T.N.$+12^h$, and the secondary magnitude of the previous tidal day if it was obtained before T.N. Since we wanted values at every mean solar hour, we found this

Table 2. Spectrum of the dynamic variation 2*A* for Oslo 1957–79

Numbers in *italics* are yearly maximum values

Year	2*A* (mb)							
	0·05	0·15	0·25	0·35	0·45	0·55	0·65	0·75
1957	10	25	84	*119*	80	34	1	0
1958	14	25	86	*121*	77	30	0	0
1959	10	28	94	*117*	77	25	2	0
1960	10	31	*105*	102	77	26	3	0
1961	7	36	87	*110*	84	28	1	0
1962	11	27	84	*105*	87	41	1	0
1963	8	27	75	*105*	93	41	5	0
1964	7	22	73	*105*	90	44	14	0
1965	5	22	68	*101*	92	51	15	0
1966	6	22	66	82	*87*	68	21	1
1967	6	20	61	77	*96*	73	20	0
1968	9	15	62	83	*92*	66	25	3
1969	6	16	60	85	*88*	70	25	4
1970	5	26	52	82	*94*	66	26	2
1971	7	23	55	78	*102*	69	17	0
1972	9	20	60	*101*	89	56	19	1
1973	9	19	69	*100*	96	44	16	0
1974	9	26	68	*112*	89	39	11	0
1975	9	31	78	*111*	84	42	0	0
1976	10	28	88	*121*	81	25	2	0
1977	15	25	94	*114*	75	26	2	0
1978	11	29	96	*113*	77	20	5	0
1979	11	28	98	*115*	74	27	0	0
Sum	204	571	1763	2359	1981	1011	231	11

Table 3. Spectrum of the dynamic variation 2*A* for Batavia 1913–22

Numbers in *italics* are yearly maximum values

Year	2*A* (mb)									
	0·10	0·30	0·50	0·70	0·90	1·10	1·30	1·50	1·70	1·90
1913	2	4	45	49	54	*83*	67	30	14	4
1914	3	5	41	52	59	69	*73*	29	19	2
1915	3	6	31	58	57	*69*	63	53	11	0
1916	3	9	28	56	54	*72*	67	50	11	0
1917	2	2	37	55	57	65	*80*	30	18	5
1918	3	0	37	56	59	62	*80*	36	17	3
1919	3	0	27	58	58	55	*74*	57	19	0
1920	3	2	24	57	57	59	*74*	59	20	0
1921	1	1	23	58	59	61	*71*	54	20	1
1922	2	0	29	53	60	59	*83*	39	21	4
Sum	25	29	322	552	574	654	732	437	170	19

by means of interpolation. Finally, the amended series $D'(t)$ was integrated to give the dynamic pressure variation $D(t)$, where t is an index marking every hour of local mean solar time (see Part I, p. 815). As mentioned above, we loose values sometimes when the moon crosses the equator and the primary and secondary maxima change position. In order to include these intervals, the missing values of $D'(t)$ were set equal to zero.

In order to compare the result with the values of $\overline{D}(v)$ shown in Fig. 2*b*, we selected the moments of tidal noon, found the nearest mean solar hour,

grouped the series $D(t)$ into 25 steps around this hour and formed the mean values. The circles in Fig. 2*b* demonstrate the result, which is a test on the two different methods. The amplitude has become somewhat higher than in curve $\overline{D}(\nu)$, but the maxima and minima are found in the same positions.

With the regular data we might ask whether it is possible to simplify the method. Instead of searching for the gradients of the pressure we might use the pressure itself and arrange the values in groups for each tidal hour. The mean values found by this method are shown by crosses in Fig. 2*b*. In the process the selection of data was restricted by the noise which was determined as before from the gradients. This procedure would be an improved Chapman–Miller method. First, the use of mean lunar time was abandoned and replaced by our tidal days defined by means of the actual position of the moon and the sun and, second, the noise was defined differently.

We notice that the dynamic pressure wave has a range of 0·75 mb as a mean during the tidal day. Haurwitz and Cowley (1969) in Table 1 reported for Batavia a dynamic amplitude of 0·082 mb. Again we have found a value considerably higher with our new method.

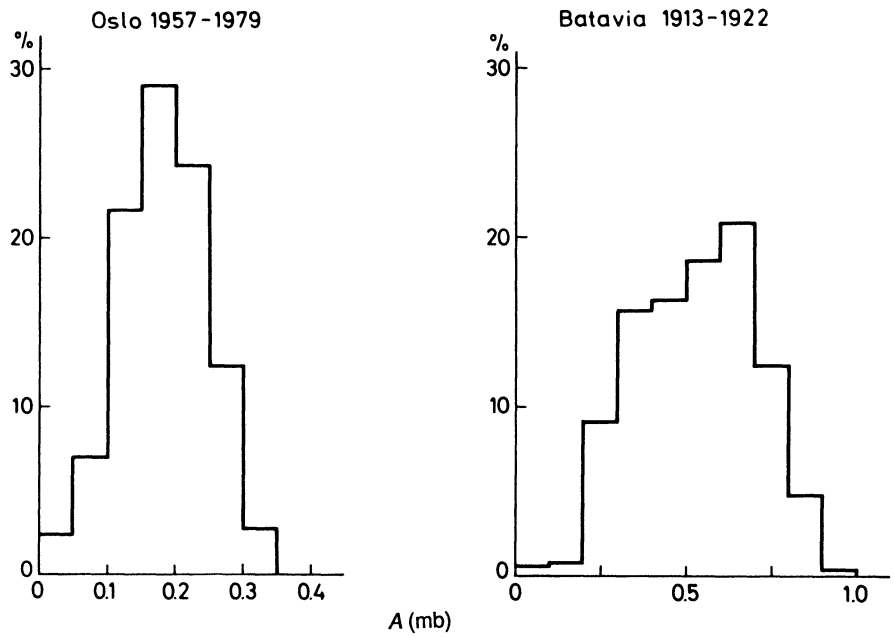

Fig. 3. Amplitude spectra of the dynamic oscillation $D(t)$: (*a*) Corrected result for Oslo (see Part II, p. 444); (*b*) Result for Batavia.

6. Spectrum of the Dynamic Variation

In Part II, Table 2, p. 443 and Fig. 3, p. 444 the amplitude spectrum of the complete daily pressure oscillation in Oslo is shown. Unfortunately, an error had been overlooked in the program, and so the correct table and figure for Oslo are presented together with a similar table and figure based on the Batavia data. Tables 2 and 3 show the spectra of the differences $2A$ between

daily maximum and minimum values of the series $D(t)$ for Oslo and Batavia respectively. In Fig. 3 we have combined the amplitude spectra for Oslo (corrected) and Batavia. In Oslo the mean daily variation has an amplitude of 0·18 mb, whereas in Batavia it has a mean of 0·52 mb. The peak values in Table 2 show that in Oslo the most frequent value of $2A$ is 0·35 mb from 1957 to 1965, increasing to 0·45 in 1966–71 and falling back to 0·35 in 1972–9. This is in agreement with the effect of the position of the node of the lunar orbit. In March 1969 the ascending node coincided with the vernal equinox and the monthly range of the moon's declination was ±28°. This means that the term $\cos^2 z$ in formula (2) of Part I varied between 0·72 and 0 during a lunar day when the declination had the extreme values. In 1960 and again in 1978 the node coincided with the autumnal equinox, the declination varied between ±18° and the term varied between 0·55 and 0·05. Consequently Table 2 shows an expected variation with the nodal cycle of 18·613 years.

A similar result could be expected for Batavia. The longitude of the node was zero in May 1913 and the range of the term was greatest that year, diminishing to a minimum in 1922. However, Table 3 shows an increase in $2A$ from 1913 to 1922. Since a smaller noise limit might alter the result the procedure was repeated from the outset with $\sigma = 0{\cdot}15$ and 0·10. The unexpected increase was removed, but the most frequent values were not decreasing from 1913 to 1922.

However, we have seen that the correlation coefficient betweeen the tidal acceleration and the gradient of the pressure yields values between −0·745 and 0·737 during the tidal day. Therefore, it is inevitable that the position of the lunar node must be important. A period of 10 years covers only half the nodal period and this is obviously not enough to show the effect. In Section 10 we also see that the dynamic and the thermal waves are more entangled in Batavia than in Oslo.

7. Importance of the Noise Limit

In Part II, Fig. 2 we demonstrated the resulting gradient of the pressure during the tidal day when the noise limit was omitted, or what is equivalent, set to 100 mb. The same procedure was followed with the Batavia data, and the result is shown in Fig. 4. Compared with Fig. 2*a*, the general form of the curve is similar, but inclusion of the remaining 4% of the data causes the errors to increase, in particlular for the values after tidal noon, exactly as seen for Oslo (Part II, Fig. 2). This could be explained as an effect of the tide on the weather but, as we shall see, it may just be the occurrence of turbulent weather during afternoon and evening.

8. 'Thermal' Oscillation of the Pressure

The gradients of the pressure were found as before, but this time they were grouped according to the hour of the day. At first they were grouped around local mean noon, but later this was improved insofar as we added the equation of time to obtain true solar hours and found the value of the gradient precisely as we found values around tidal noon in the search for the dynamic effect. The difference between the use of mean or true solar time was small, but we prefer to use the latter in the following.

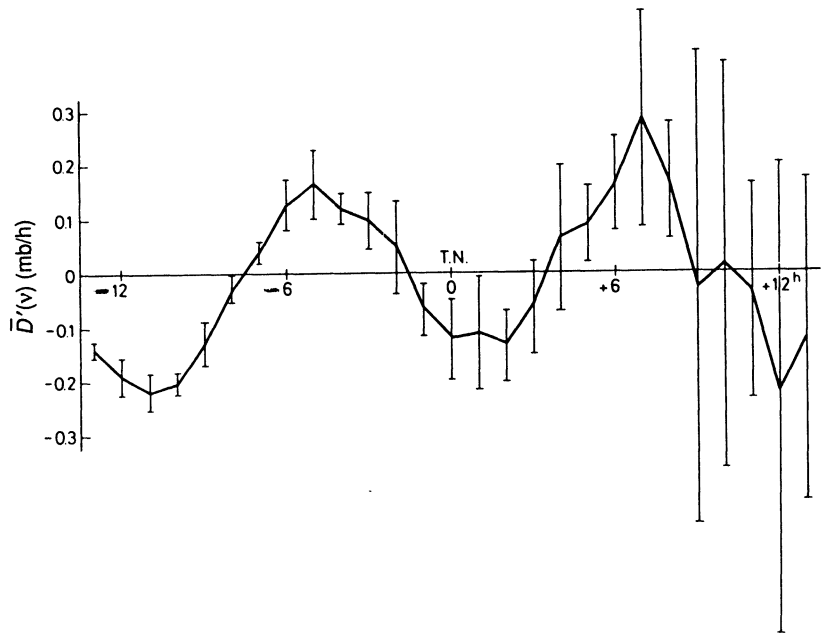

Fig. 4. Mean values of the gradient of the pressure $\overline{D}'(\nu)$ when the noise test is omitted.

The method described in Part I, pp. 819–21 was pursued and monthly means of the daily variation of the series $T(t)$ are shown in Table 4. The last column shows the yearly mean. This table can be compared with v. Hann (1919, p. 477) where Batavia data for the years 1866–1905 were presented. We remark that v. Hann's result reveals a higher maximum at 9 h (+0·23 mb) and a lower minimum at 15 h (−0·28 mb). Apart from this the two results agree very well.

Since our method was based on the determination of the function $\overline{T}'(\nu)$ by a procedure similar to the determination of the dynamic gradient $\overline{D}'(\nu)$, we could also integrate $\overline{T}'(\nu)$ to find $\overline{T}(\nu)$ by means of the same Fourier method. This resulted in a 24-hour period with mean amplitude 0·843 mb and a 12-hour period with amplitude 1·209 mb.

In Fig. 5 we show the resulting 'thermal' variation with the solid curve and the 24- and 12-hour components with dashed lines. The sum of the higher harmonics results in variations of ±0·038 mb around a mean value of −0·007 mb. However, we also used the simpler method of grouping the actual pressure data according to the hour of the day. Local mean solar time was used, and the noise limitation was omitted. Now, the yearly mean of the daily variation shown by the crosses and dashed curve in Fig. 6 agrees to 0·02 mb with the results of v. Hann. This means that the simple method of summing the pressure values directly in groups for each hour of the day, without regard to noise, may lead to a somewhat enlarged amplitude.

For the series $D(t)$ we realised that it was possible to use a modified method where the gradients were only used to determine noise, and the pressure was

Table 4. Monthly means of the daily pressure variation *T(t)*

H	Jan.	Feb.	Mar.	Apr.	May	Jun.	Jul.	Aug.	Sep.	Oct.	Nov.	Dec.	Year
0	0·72	0·86	0·90	0·86	0·79	0·80	0·82	0·85	0·79	0·63	0·57	0·62	0·77
1	0·22	0·35	0·35	0·32	0·31	0·37	0·41	0·37	0·25	0·08	0·01	0·11	0·26
2	−0·20	−0·11	−0·12	−0·11	−0·13	−0·02	0·03	−0·01	−0·10	−0·28	−0·37	−0·27	−0·14
3	−0·50	−0·45	−0·46	−0·40	−0·43	−0·31	−0·25	−0·26	−0·29	−0·44	−0·55	−0·51	−0·40
4	−0·57	−0·57	−0·56	−0·49	−0·47	−0·35	−0·29	−0·30	−0·29	−0·34	−0·46	−0·50	−0·43
5	−0·35	−0·43	−0·42	−0·35	−0·28	−0·18	−0·13	−0·13	−0·06	−0·04	−0·13	−0·22	−0·23
6	0·11	−0·09	−0·09	0·02	0·09	0·14	0·18	0·25	0·37	0·43	0·37	0·27	0·17
7	0·69	0·44	0·42	0·54	0·58	0·59	0·65	0·76	0·91	0·97	0·92	0·82	0·69
8	1·17	1·02	0·97	1·03	1·04	1·04	1·12	1·26	1·35	1·38	1·30	1·22	1·16
9	1·37	1·36	1·34	1·32	1·25	1·22	1·33	1·48	1·51	1·42	1·32	1·32	1·35
10	1·23	1·34	1·36	1·25	1·09	1·01	1·13	1·27	1·26	1·10	1·00	1·07	1·18
11	0·83	1·03	1·02	0·79	0·60	0·52	0·61	0·69	0·63	0·50	0·44	0·56	0·68
12	0·30	0·52	0·45	0·17	0·02	−0·02	0·06	0·06	−0·08	−0·20	−0·22	−0·02	0·08
13	−0·38	−0·18	−0·30	−0·55	−0·65	−0·65	−0·59	−0·64	−0·82	−0·97	−0·95	−0·70	−0·62
14	−1·16	−0·99	−1·14	−1·34	−1·36	−1·32	−1·30	−1·40	−1·56	−1·66	−1·64	−1·40	−1·36
15	−1·74	−1·62	−1·73	−1·86	−1·77	−1·70	−1·74	−1·88	−2·00	−2·02	−1·98	−1·83	−1·82
16	−1·94	−1·95	−1·95	−1·94	−1·76	−1·72	−1·81	−1·96	−2·05	−1·99	−1·87	−1·83	−1·90
17	−1·68	−1·83	−1·75	−1·61	−1·41	−1·43	−1·56	−1·70	−1·73	−1·56	−1·36	−1·43	−1·59
18	−1·08	−1·29	−1·20	−1·04	−0·88	−0·94	−1·10	−1·21	−1·14	−0·87	−0·65	−0·79	−1·01
19	−0·37	−0·58	−0·51	−0·34	−0·25	−0·33	−0·51	−0·56	−0·42	−0·13	0·07	−0·09	−0·33
20	0·29	0·09	0·17	0·36	0·42	0·32	0·14	0·13	0·28	0·53	0·69	0·53	0·33
21	0·82	0·70	0·77	0·91	0·93	0·83	0·71	0·71	0·84	1·05	1·13	0·96	0·86
22	1·13	1·14	1·19	1·21	1·15	1·06	1·02	1·07	1·16	1·28	1·27	1·13	1·15
23	1·10	1·23	1·28	1·24	1·12	1·05	1·07	1·15	1·18	1·14	1·08	1·00	1·14

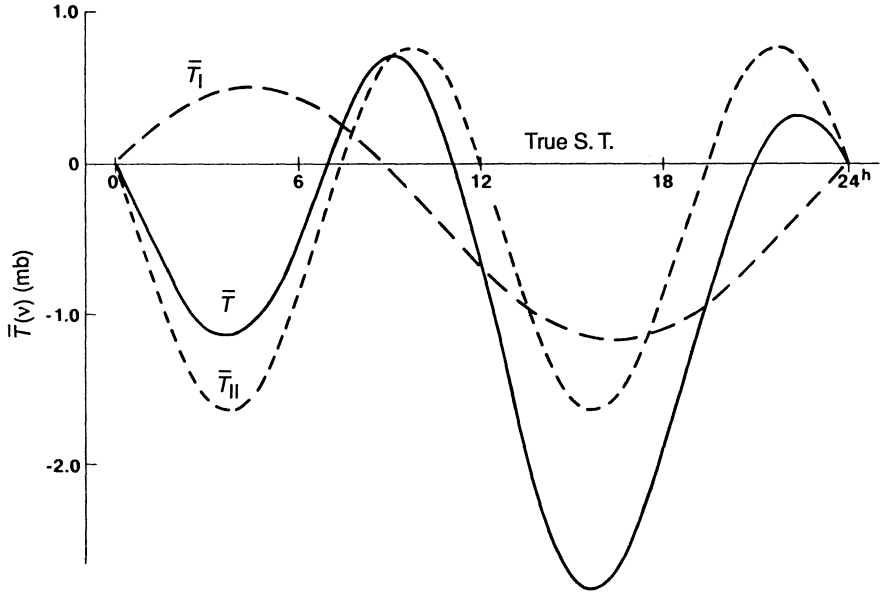

Fig. 5. Variation of mean 'thermal' pressure $\overline{T}(\nu)$ around true noon, showing its harmonic components $\overline{T}_I$ and $\overline{T}_{II}$.

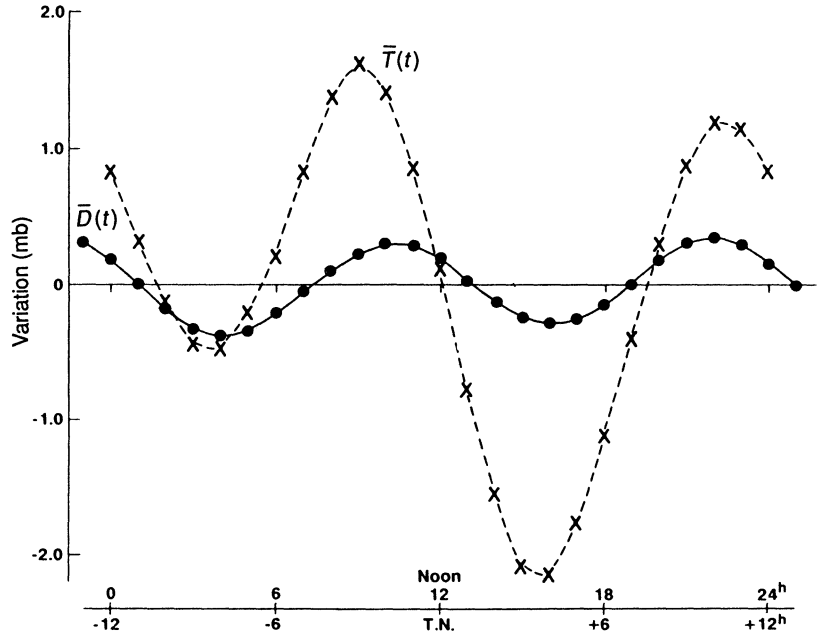

Fig. 6. Circles and the solid curve show the dynamic variation around tidal noon, determined directly from the pressure values without noise limitation. Crosses and the dashed curve show the 'thermal' variation during the mean solar day, also determined directly from pressure values without noise limit.

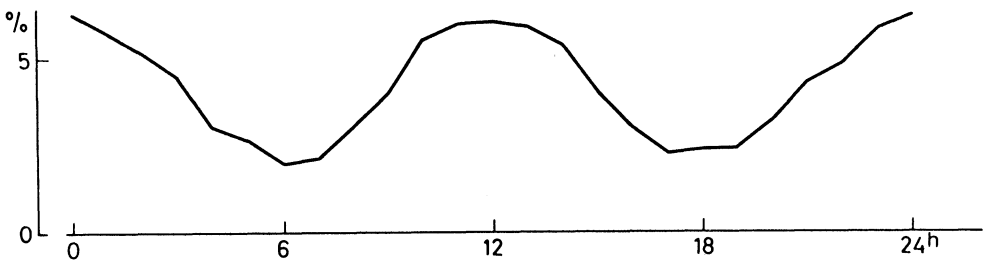

Fig. 7. Distribution of tidal noon (T.N.) according to time of day.

found directly from the data. Now this has been repeated, but without the noise limitation. In Fig. 6 the result is shown by the circles and solid curve.

9. Separation of the Dynamic and 'Thermal' Variation

In Fig. 4 we saw that inclusion of all data without noise limitation might be interpreted as turbulent pressure prevailing during the 'tidal afternoon and evening'. However, if we arrange the occurrence of tidal noon according to the times of day, we find a distribution with two maxima, at midnight and midday as shown in Fig. 7. If we also account for the 'magnitudes' of the acceleration the clustering around midnight and midday becomes still more prominent (cf. spring tide). Therefore, the result shown in Fig. 4 is probably due to the effect of the inclusion of more turbulent weather in the afternoon and evening.

10. Statistical Tests

In Parts I (p. 816) and II (p. 447) we introduced statistical tests. Similar tests were made on the Batavia result. With $O(t)$ as the series of the observed pressure we produced a series $O(t)$–$D(t)$ and used this series instead of $O(t)$ as the data in the search for new values of $\overline{D}'(v)$, assuming that we would find a statistically zero result. This was not the case, in contrast to the analogous tests for Oslo, shown in Part II, Table 4. The same happened when we introduced a dataset $O(t)$–$T(t)$ in the search for the 'thermal' gradient $\overline{T}'(v)$.

We also tried the use of datasets of the form $O(t)-aT(t)-bD(t)$ in an attempt to find values of a and b which would reduce the oscillations of new values of $\overline{D}'(v)$ and $\overline{T}'(v)$ below the standard deviation. The values of the gradients were reduced considerably with $a=0\cdot7$, $b=0\cdot3$ or $a=0\cdot9$, $b=0\cdot9$ in the two cases, but were not below the standard deviation. The explanation may be that in Batavia the two effects are more entangled.

However, it was possible to perform an entirely independent test on the importance of the series $D(t)$. The difference between the maximum and the minimum pressure for each mean solar day was found and the values sorted according to the lunar phase. Fig. 8 shows the result. The daily variation of the pressure has the smallest values 2–3 days after the new moon and

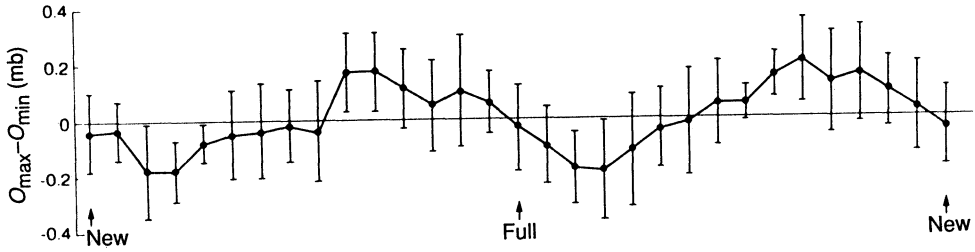

Fig. 8. Range of daily variation $O_{max} - O_{min}$ as a function of lunar phase.

full moon, and the largest values 2–3 days after the first and third quarter. The uncertainty marked by the error bars is of course fairly high and could only be reduced by means of a longer data series. But as we have seen, the pressure variation during a tidal day depends on the 'magnitude' of the tidal acceleration which is largest around new and full moon. In Fig. 8 we notice an increase of the amplitudes from the new and full phase to the quarter phases, which may be interpreted as an augmenting dynamic wave.

11. The Moon and the Weather

In Part I we raised this question and referred to Adderly and Bowen (1962) and Bradley *et al.* (1962). Recently Currie and O'Brien (1988) have shown that records of the yearly total precipitation in the north-eastern United States are highly correlated with the tidal maxima of the 18·6 year lunar tide, and also with the sunspot cycle.

12. Conclusions

We have shown that the values of the dynamic atmospheric tides inherent in the pressure records from Oslo and Batavia reach values many times higher than the amplitudes referred to by Haurwitz and Cowley (1969). In records from Japan, Currie (1982) has found amplitudes between 0·1 and 0·3 mb. Currie (1987) gave samples worldwide but erred by reducing to unit variance, thus losing units. Currie (personal communication, 1990) reprocessed all the data and found that amplitudes of the 18·6 year term reach as high as 0·5 mb in parts of South America and the USSR. Currie and O'Brien (1988, p. 274) also discussed the physical mechanism in terms of Doodson's (1922) development of the tidal potential. They quoted the ratio $M_N/M_2 = 0{\cdot}036$, where M_N is Doodson's constant for the longitude of the lunar node and M_2 is the lunar half-day constant. However, with reference to Haurwitz and Cowley's value of 0·08 mb for M_2 in Indonesia, they concluded that the M_N term in pressure is an order of magnitude larger than that for M_2.

It is true that Doodson's method, and the more precise revision by Bartels (1957), can be used to compute the tidal acceleration if all terms are included. However, as we have shown, this does not support the idea of using mean lunar time to search for the tidal wave.

Our method differs from Doodson's mainly because we do not develop series based primarily on the mean lunar day. The moon and the sun do

not circle the earth in the plane of the equator at constant distances. We have treated the tidal forces as quasiperiodic entities and developed a method where the principal variable $\cos^2 z$, with z the zenith distance, is made use of in the study. The extreme value of the moon's declination varies between ±18° and ±28° with the nodal cycle of 18·613 years, and it is not surprising that this cycle must be important.

In Parts I and II we used the word 'thermal' in connection with the oscillation which is connected with the time of day, but part of which must of course be caused by the exclusive solar dynamic tide. The argument that this may be the cause of the semi-diurnal variation has formerly been dismissed by the smallness of the hitherto discovered dynamic variation, of which only about one-third is caused by the sun (see Chapman and Lindzen 1970, pp. 10–11).

The explanation so far has been a possible free resonance period of the atmosphere of 12 hours. Now we have seen that the dynamic variation attains much higher values than that determined by the old method. We have also demonstrated that the quasiperiodic tidal noon has a tendency to cluster around midnight and midday. Therefore, it is possible that the 'thermal' 12-hour variation is induced by the complete lunisolar dynamic tide.

References

Adderly, E. E., and Bowen, E. G. (1962). *Science* **137**, 749–50.
Bartels, J. (1957). *Handbuch d. Phys.* **48**, 734–74.
Bradley, D. A., *et al.* (1962). *Science* **137**, 748–9.
Brahde, R. (1988). *Aust. J. Phys.* **41**, 807–31.
Brahde, R. (1989). *Aust. J. Phys.* **42**, 439–50.
Chapman, S., and Lindzen, R. S. (1970). 'Atmospheric Tides' (Reidel: Dordrecht).
Currie, R. G. (1982). *Geophys. J. R. Astron. Soc.* **69**, 321–7.
Currie, R. G. (1987). *In* 'Climate, History, Periodicity and Predictability' (Eds M. R. Rampino *et al.*), pp. 379–403 (Van Nostrand Reinhold: New York).
Currie, R. G., and O'Brien, D. P. (1988). *J. Climatol.* **8**, 255–81.
Doodson, A. T. (1922). *Proc. R. Soc. London* **100**, 305–29.
Hann, J. v. (1919). *Sitzb. Akad. Wiss. Wien Abt. IIa* **128**, 379–506.
Haurwitz, B., and Cowley, A. D. (1969). *Pure Appl. Geophys.* **6**, 122–50.

Manuscript received 18 June, accepted 21 August 1990